Contrib Mineral Petrol (1993) 114:53–62

Contributions to Mineralogy and Petrology

Pre-eruptive melt composition and constraints on degassing of a water-rich pantellerite magma, Fantale volcano, Ethiopia

James D. Webster[1] *, Richard P. Taylor[2], and Christine Bean[3]

[1] Department of Mineral Sciences, American Museum of Natural History, Central Park West at 79th Street, New York, NY 10024-5192, USA
[2] Department of Earth Sciences, Carleton University, Ottawa, Ontario Canada K1S 5B6
[3] McCrone Associates-Atlanta, 1412 Oakbrook Drive, Suite 100, Norcross, Georgia 30093, USA

Received June 11, 1992 / Accepted October 23, 1992

Abstract. To determine the pre-eruptive composition of peralkaline magma at Fantale volcano, Ethiopia, we have studied glass inclusions in phenocrysts from a late-erupting, glassy pantelleritic lava flow. Matrix glass and crystal-free glass inclusions in quartz were analyzed for all major and most minor elements by electron microprobe and for H_2O and 15 lithophile trace elements by ion microprobe (SIMS). Compositions of inclusions may have been slightly modified by post-trapping quartz crystallization, the average concentrations of all constituents but silica may be artificially high by 10% relative. Glass inclusions contain extreme enrichments in H_2O (mean of 4.6 to 4.9 wt%) and several lithophile trace elements, which suggest that the lava erupted from a highly evolved, water-rich fraction of magma. The pre-eruptive concentration of water was much higher than that generally considered to occur in pantellerite magmas. Trends observed for lithophile elements in whole-rock samples from pre-, syn- and post-caldera eruptive units are mimicked in glass inclusions from the studied pantellerite lava; concentrations of Rb, Y, Zr, Nb, and Ce $\pm$ Cl increase with progressive differentiation. With the exception of Cl and H_2O contents, the composition of matrix glass is similar to that of glass inclusions suggesting: that few constituents exsolved from magma or cooling glass; eruption and quench of the lava occurred rapidly; and the matrix glass is, largely, compositionally representative of melt. Higher average abundances of Cl and H_2O in glass inclusions suggest that these volatiles exsolved after melt entrapment; degassing could have occurred as either an equilibrium or disequilibrium process.

Introduction

Pantellerites and comendites erupt from chemically evolved, silicic, peralkaline magma. Indirect evidence (Nicholls and Carmichael 1969; Macdonald and Bailey 1973; Mahood 1981, 1984; Bailey and Macdonald 1987; Bailey and Hampton 1990) suggests that pantelleritic magmas contain relatively low concentrations of water prior to eruption. The principal supporting arguments include: (1) low concentrations of water in associated matrix glasses; (2) strong Cl enrichments in matrix glasses suggesting that a Cl-rich aqueous vapor could not have exsolved and left behind a Cl-rich melt; (3) comparison of phase assemblages and phase compositions observed in natural pantellerites with those in anhydrous and water-saturated experiments involving pantellerite melt. Recent studies (Kovalenko et al. 1988, 1990; Lowenstern et al. 1991; Lowenstern and Mahood 1990, 1991) have attempted to estimate pre-eruptive volatile abundances of pantelleritic magmas directly by determining the composition of glass inclusions in phenocrysts, which presumably preserve pre-eruptive concentrations of volatiles. The results indicate that the analysis of glass inclusions is, at present, the most reliable means of constraining pre-eruptive volatile concentrations of volcanic systems. Glass inclusions from Pantelleria, for example, contain from 1.39 $\pm$ 0.05 wt% (Lowenstern and Mahood 1991) to 4.3 $\pm$ 0.2 wt% H_2O (Kovalenko et al. 1988).

Water and other volatiles in magma drive volcanic eruptions (Sparks 1978; Blake 1984; Civetta et al. 1988), and it has also been suggested that fluids may play a significant role in the genesis and differentiation of some peralkaline magmas (Ewart et al. 1968; Bailey and Macdonald 1975, 1987; Macdonald et al. 1987; Bailey and Hampton 1990). Before volcanologists can understand the role of aqueous fluids in magmatic differentiation and volcanic eruption, it is essential to: (1) estimate the pre-eruptive abundances of volatile constituents in the magma; (2) determine the extent to which water and other relatively mobile elements are lost from magma and obsidian during and after eruption. In this regard, we have determined the pre-eruptive concentrations of 12 major and minor elements (including H_2O) and 15 lithophile trace elements in a post-caldera, pantelleritic lava flow from Fantale volcano, Ethiopia, by analyzing glass inclusions in phenocrysts. The compositions of glass inclusions

Correspondence to: J.D. Webster

are compared with those of matrix glasses to assess the mobility of volatiles after melt entrapment and during/after eruption. The data are also compared with the results of experiments to understand the relative importance of equilibrium versus disequilibrium degassing at Fantale.

Geological background

Fantale is a Quaternary stratovolcano located at the northern end of the Ethiopian rift valley (Mohr 1970). Tuffs and lava flows of pantelleritic composition (Lacroix 1930; Teillhard deChardin and Lamare 1930; Rohleder and Hitchen 1930; Gibson 1970) were erupted from a zoned magma chamber (Dickinson and Gibson 1972; Gibson 1974). The pre-caldera volcanic rocks include trachyte, rhyolite, and obsidian flows with rare intercalated pumiceous tuffs. Late pre-caldera eruptive units include glassy, sanidine-aenigmatite-phyric lava flows; the caldera-forming eruptive units are welded ash-flow tuffs. Post-caldera rocks include trachyte flows and glassy pantelleritic lava flows. For the present study, we analyzed matrix glass and glass inclusions from two obsidian samples, AW-13 and AW-14, collected within the caldera from a post-caldera, quartz-phyric pantellerite lava flow.

The two samples are similar petrographically, consisting of approximately 14 vol% phenocrysts of anorthoclase, aenigmatite, quartz, ferrohedenbergite, and opaques in a non-hydrated, green glass matrix also containing microphenocrysts of anorthoclase and aenigmatite. The phenocryst compositions are very similar to those in pantellerites from Pantelleria (Carmichael 1962; Mahood and Stimac 1990), the only significant differences being that aenigmatites and pyroxenes from Fantale contain more Na_2O and less Al_2O_3 (Richard P. Taylor, unpublished data).

Methods

Sample preparation

Both samples were disaggregated gently, with a steel mortar and pestle, to avoid crushing the phenocrysts. Hand-picked separates of quartz, aenigmatite, and anorthoclase phenocrysts were washed in cold, concentrated HF for approximately 30 minutes to remove attached glass from the exterior of grains, which were then mounted on glass slides. The grain mounts were ground with 320 grit SiC paper until several glass inclusions were exposed on the surface; then the mounts were polished with alumina slurries. The polished grain mounts were cleaned with ethanol and were carbon-coated for electron microprobe analysis and gold coated for ion microprobe analysis.

Methods of analysis

Glass inclusions ≥ 5 micrometers (μm) in diameter, in quartz and anorthoclase phenocrysts, and matrix glass were analyzed for SiO_2, Al_2O_3, Na_2O,K_2O, FeO, MgO, CaO, TiO_2, MnO, F, and Cl with an ARL-SEMQ electron microprobe using wavelength-dispersive analysis. The analytical methods are described in Webster (1992). Crystal-bearing glass inclusions were not analyzed. The electron beam was defocused as much as possible to reduce alkali element migration during analysis. The accuracy and precision of the electron microprobe analyses were determined by conducting replicate analyses of two rhyolitic glasses of known composition (Table 1) during each analytical session.

The concentrations of H_2O, Li, Be, B, Rb, Sr, Y, Zr, Nb, Cs, Ce, U, Th, Mo, W, and Sn in matrix glass and glass inclusions > 15 μm in diameter, in quartz, were determined by secondary ion mass spectrometry (SIMS) using Cameca IMS 4f ion microprobes; methods are described in Webster and Duffield (1991). One glass inclusion located in feldspar was also analyzed for H_2O.

Table 1. Precision and accuracy of electron microprobe analyses

Element	Spor Mountain glass[a]			Big Southern Butte obsidian[b]		
	Other analysis (wt%)	Microprobe analysis[c] (wt%)	Microprobe precision[d] (relative%)	Other analysis (wt%)	Microprobe analysis[e] (wt%)	Microprobe precision[d] (relative%)
SiO_2	70.13	70.84	0.4	75.57	75.74	0.3
Al_2O_3	13.55	13.70	0.9	12.41	12.36	0.3
CaO	0.40	0.37	3	0.48	0.47	6
Na_2O	4.44	4.13	2	4.30	4.32	3
K_2O	4.76	4.95	1	4.62	4.59	2
FeO	n.d.[f]	n.d.[f]	n.d.[f]	1.59	1.42	6
MgO	n.d.[f]	0.04	25	0.00	0.01	100
TiO_2	.03	0.03	33	0.09	0.09	11
MnO	.06	0.06	33	0.04	0.03	33
F	1.25	1.25	14	0.32	0.27	30
Cl	0.15	0.15	5	0.20	0.20	4

Comparison of replicate electron microprobe analyses of two "known-unknown" glasses with their compositions as determined by X-ray fluorescence and/or various wet chemical techniques; analytical techniques are described in (Webster and Duffield 1991). Microprobe analyses were conducted with an ARL-SEMQ at the American Museum of Natural History during two analytical sessions. MgO, TiO_2, and MnO exhibit comparatively large precisions inasmuch as concentrations of these elements are near detection limits.

[a] Spor Mountain glass was prepared from natural (metaluminous) topaz rhyolite powder SM-1 fused with roughly 5 wt% H_2O in a sealed Pt capsule at roughly 1,000°C and 3 kbar; nearly all iron was lost to Pt capsule during fusion. Analytical techniques are described by Webster et al. (1987)

[b] Big Southern Butte obsidian is a relatively dry peralkaline glass. Analytical techniques are described by Macdonald and Bailey (1973)

[c] Mean concentrations for 4 analyses.

[d] One σ deviation about the means (% relative)

[e] Mean concentrations for 6 analyses

[f] No data (n.d.)

Matrix effects are a major concern for SIMS analysis of glasses having different bulk compositions. The H_2O standards used in this study include *metaluminous* haplogranite and quartz-orthoclase glasses containing up to 7 wt% H_2O and natural, *peraluminous* and *peralkaline* obsidian samples containing < 1 wt% H_2O. The peralkaline obsidian samples contain from 1–3 wt% FeO and 0.1–0.3 wt% H_2O. For accurate SIMS analyses it is essential to determine whether metaluminous glasses and peralkaline glasses of varying water contents exhibit similar ion yields (described in Webster and Duffield 1991) for water and lithophile trace elements. The ion yields for the major elements Al, Na and K in the glass inclusions and matrix glasses were determined during each SIMS analysis, and it has been determined (Webster and Duffield 1991; J. D. Webster unpublished data) that the ion yields for Al range from 1.7 to 2.4, those for Na range from 0.7 to 1.2, and those for K range from 0.7 to 1.3 in all standard glasses. If the ion yields of major elements in the glass inclusions are within the ranges determined for the standard glasses, then we assume that the water and trace-element analyses are not adversely influenced by matrix effects, and the analyses are deemed accurate. All constituents in the glasses were analyzed as high-energy ions to minimize the effects of mass interferences and reduce matrix effects. Only secondary ions with energies in the 78 ± 20 eV range were analyzed. The result is that 76% of the SIMS analyses for the peralkaline matrix glasses and glass inclusions conducted for this study gave ion yields for Al, Na, and K that are within these ranges. The other analyses gave slightly lower ion yields for Na and K, because the "burn-in" time for the primary ion beam was longer than that normally used. Hence, the analyzed inclusions giving slightly lower ion yields may include apparent water and trace-element contents that are artificially low to a small degree.

The precision of the ion microprobe analyses has been approximated by replicate analyses of two glass inclusions (Table 2). Determination of analytical precision and accuracy is particularly important given that two ion microprobe were used. As shown in Table 2, glass inclusion 15 was analyzed in two spots for a total of four analyses at McCrone Associates-Atlanta; glass inclusion 1 was analyzed twice in one spot at McCrone Associates-Atlanta and twice in another spot at Edinburgh. The intra-and inter-instrument reproducibility of the two ion microprobes is good. The 1σ precision of the H_2O analyses is very good (i.e. ≤ 9% relative), and the precision for the analyses of Li, Be, B, Rb, Y, Zr, Nb, Cs, and Ce in the inclusions is good (i.e. ≤ 15% relative). The precision for Sr and Th ranges from 15 to 20% relative; the precision for Mo, Sn, W, and U is relatively poor and is largely the result of poor counting statistics. This technique of estimating the precision assumes that the entrapped glass is homogeneous; otherwise, some component of the irreproducibility is a result of sample heterogeneity and the reported precisions are artificially high.

Results

Textural characteristics of the glass inclusions

Glass inclusions occur in quartz, anorthoclase, and aenigmatite phenocrysts. Those in aenigmatite are rare and typically contain apatite microphenocrysts; they are not discussed further.

Glass inclusions in anorthoclase are generally small, ≤ 25 μm in diameter, and many are variably devitrified. One contains amphibole microphenocrysts that project from the inclusion margin into glass, suggesting that they crystallized after entrapment. Most glass inclusions in feldspar are elongate with long dimensions parallel to cleavage. Many inclusions occur along cracks and contain multiple bubbles, suggesting that they leaked volatiles along cleavage planes and no longer reflect the pre-eruptive composition of melt. Glass inclusions in anorthoclase are less abundant than in quartz. Because of their relative scarcity and their tendency to occur along cracks in host grains, few glass inclusions in feldspar were analyzed.

Many glass inclusions in quartz phenocrysts contain multiple inclusions, and most inclusions range from less

Table 2. Analytical precision for SIMS analyses

Element	Inclusion 1[a]		Inclusion 15[b]	
	Average concentration (ppm)	Analytical precision[c] (% relative)	Average concentration (ppm)	Analytical precision[c] (% relative)
H (as H_2O)	38,000	7	50,000	9
Li	69	9	69	6
Be	9.3	11	10.4	3
B	17	10	22	14
Rb	179	13	189	13
Sr	9.8	16	6.8	26
Y	162	6	143	6
Zr	1950	8	1637	5
Nb	240	4	194	7
Mo	9.9	20	11.5	16
Sn	30	32	24	17
Cs	3.1	10	2.4	13
Ce	360	4	272	4
W	7.4	45	5.6	29
Th	14.4	8	15.5	17
U	3.7	46	5.3	25

Precisions determined by repeat analyses of two glass inclusions

[a] Inclusion 1 was analyzed twice with a Cameca 4f ion microprobe at the University of Edinburgh and twice with a Cameca 4f at McCrone Associates-Atlanta

[b] Inclusion 15 was analyzed four times during two analytical sessions with a Cameca 4f ion microprobe at McCrone Associates-Atlanta

[c] The ± 1σ about the mean is in % relative

than 1 to 120 μm on a side. The shapes of the glass inclusions are either square, rectangular, or nearly perfect negative crystals of quartz; the corners within inclusions are always rounded. Most inclusions do not appear to be in contact with cracks or fractures. Glass inclusions are much more abundant in quartz from sample AW-14 than in sample AW-13. Roughly three-fourths of the quartz grains picked at random from sample AW-14 contain at least one glass inclusion; whereas, approximately one-half of the quartz grains from AW-13 contain inclusions. Glass inclusions from sample AW-13 are clear to light brown in color, and no crystals were observed within trapped glass. Glass inclusions from sample AW-14 are light to dark brown in color. Most contain no crystals, while darker inclusions contain distinct, sub-micron-sized minerals in glass.

Most glass inclusions in quartz contain a single bubble, and about 15–20% of those studied contain multiple bubbles. Most bubbles contain sub-micron-sized crystals of an unidentified birefringment mineral. Bubbles typically make up 1–3 vol% of inclusions; however, the total volume of bubbles in glass inclusions that contain either large or multiple bubbles may approach 20%. Relatively large bubble volumes may be the result of vapor saturation in addition to glass shrinkage during cooling.

Composition of the glass inclusions

Concentrations of major and minor elements were determined for 23 glass inclusions in quartz from sample AW-14 and 24 inclusions in quartz from AW-13. The mean concentrations of major and minor elements in glass inclusions from both samples are very similar to each other and are chemically equivalent to pantellerite melt. Eight inclusions from sample AW-14 and nine inclusions from AW-13 were large enough to analyze for trace elements and H_2O by SIMS; we report only the compositions of inclusions analyzed by SIMS (Tables 3 and 4). The results of SIMS analyses show that the concentrations of most trace elements vary by a factor of 2.

The water concentrations range from 0.4 to 8.5 wt%, and are high on average. Even though the full range is quite large, the great majority of the inclusions in quartz exhibit a relatively limited range of water contents (Fig. 1). The average abundance of H_2O in glass inclusions from both samples is 4.8 wt%; 84% of the inclusions contain water concentrations that are within $\pm 3\sigma$ of the average. High water contents are compatible with relatively low electron microprobe totals (Table 3). The low totals indicate that an essential constituent (or constituents) was not detected during electron microprobe analysis, and the SIMS data suggest that the predominant missing constituent was H_2O.

Some of the analyzed glass inclusions occur along cracks in the host phenocryst, but the cracks must have formed after the inclusions were quenched because there is no evidence of volatile loss; their compositions are not recognizably different from that of other glass inclusions or of the average inclusion compositions. The data suggest, however, that at least one inclusion may have lost

Table 3. Composition of glass inclusions[a] located in quartz phenocrysts from Fantale samples AW-13 (analyses 1 through 9) and AW-14 (analyses 10 through 17). SiO_2 through H_2O in wt%[b], and Li through U in ppm[c]

	1	1[d]	2	3	4	5	6	7	8	9
Total	94.18	94.18	95.31	94.03	97.42	93.78	92.57	95.68	97.44	96.30
SiO_2	70.98	70.98	70.80	70.64	70.04	71.54	71.51	72.73	71.44	71.12
Al_2O_3	8.57	8.57	8.99	8.34	8.80	9.41	8.66	8.96	8.57	8.57
CaO	0.36	0.36	0.32	0.37	0.38	0.32	0.35	0.28	0.31	0.30
Na_2O	6.70	6.70	6.74	6.50	6.88	6.61	6.51	6.46	6.27	6.39
K_2O	4.41	4.41	4.28	4.44	4.32	4.13	4.13	3.94	4.60	4.67
FeO	7.72	7.72	7.62	8.30	8.27	6.98	7.63	6.67	7.59	7.72
MgO	0.00	0.00	0.00	0.02	0.06	0.07	0.06	0.04	0.07	0.05
TiO_2	0.29	0.29	0.27	0.32	0.25	0.26	0.26	0.24	0.31	8.27
MnO	0.34	0.34	0.27	0.38	0.34	0.25	0.26	0.24	0.39	0.37
F	0.37	0.37	0.44	0.44	0.36	0.17	0.36	0.18	0.16	0.21
Cl	0.30	0.30	0.32	0.31	0.32	0.27	0.29	0.27	0.29	0.33
H_2O	3.60	4.00	4.50	6.30	3.90	4.80	5.30	4.10	4.70	4.40
Li	63.0	74.0	35.0	109.0	44.0	54.0	68.0	48.0	80.0	70.0
Be	8.8	9.8	10.5	8.4	11.4	11.4	10.9	8.2	9.9	10.9
B	19.0	15.6	21.0	21.0	22.5	20.6	23.3	22.7	26.0	30.0
Rb	166.0	196.0	194.0	237.0	202.0	182.0	214.0	369.0	202.0	239.0
Sr	8.2	11.3	9.2	7.2	5.3	2.5	7.8	13.1	9.3	12.8
Y	164.0	160.0	180.0	236.0	162.0	158.0	163.0	230.0	144.0	168.0
Zr	2,044.0	1,856.0	2,334.0	2,801.0	1,593.0	1,906.0	1,870.0	2,722.0	1,632.0	1,976.0
Nb	244.0	235.0	279.0	302.0	215.0	162.0	208.0	344.0	221.0	230.0
Mo	8.0	11.8			10.8	5.5	7.2	9.8	5.9	13.0
Sn	38.0	21.4			26.0	21.0	19.0	28.0	18.0	24.5
Cs	3.0	3.2	3.0	2.0	3.4	2.5	2.9	5.5	3.6	2.6
Ce	365.0	354.0	389.0	444.0	305.0	342.0	349.0	431.0	296.0	280.0
W	6.0	8.8			9.5	5.5	7.5	6.1	8.3	6.5
Th	11.0	15.0	6.0	20.0	11.7	15.2	13.0	22.5	13.0	12.0
U	2.0	5.4			5.4	2.9	3.8	7.2	4.7	5.0

Table 3 (continued)

	10	11	12	13	14	15	15[d]	16	17
Total	94.35	99.55	95.55	94.5	94.75	95.65	95.43	93.79	97.92
SiO_2	71.99	72.84	70.63	70.55	71.16	72.19	71.42	70.11	69.47
Al_2O_3	8.16	8.29	8.22	9.39	8.78	8.39	8.46	8.90	9.94
CaO	0.35	0.32	0.36	0.35	0.31	0.32	0.33	0.35	0.28
Na_2O	6.57	6.59	6.83	6.37	6.88	6.83	7.21	7.22	7.60
K_2O	4.23	3.87	4.38	4.49	4.15	3.95	4.02	4.38	4.32
FeO	7.57	7.06	8.26	7.66	7.61	7.24	7.37	7.87	7.32
MgO	0.03	0.01	0.00	0.03	0.04	0.04	0.03	0.05	0.04
TiO_2	0.24	0.25	0.26	0.31	0.29	0.28	0.24	0.31	0.23
MnO	0.32	0.29	0.35	0.32	0.29	0.29	0.28	0.34	0.25
F	0.34	0.23	0.44	0.25	0.17	0.23	0.39	0.18	0.22
Cl	0.29	0.26	0.34	0.31	0.30	0.26	0.25	0.29	0.33
H_2O	4.20	0.40	8.50	4.10	4.30	5.20	4.80	3.90	4.30
Li	65.0	38.0	100.0	89.0	68.0	72.0	65.0	62.0	58.0
Be	8.6	7.2	10.7	9.9	10.6	10.4	10.4	10.6	11.6
B	16.0	15.0	22.0	20.0	22.0	21.0	23.0	20.0	27.0
Rb	192.0	161.0	188.0	215.0	181.0	180.0	197.0	150.0	216.0
Sr	9.7	7.7	10.4	9.4	8.9	8.6	5.0	6.6	7.5
Y	162.0	171.0	212.0	223.0	155.0	147.0	139.0	143.0	173.0
Zr	2,182.0	2,248.0	2,347.0	2,620.0	2,137.0	1,653.0	1,621.0	1,519.0	2,673.0
Nb	248.0	231.0	268.0	273.0	236.0	201.0	186.0	218.0	300.0
Mo		5.0			10.5	10.1	12.8	10.4	11.0
Sn		28.0			24.0	22.0	26.0	21.0	27.0
Cs	2.0	4.0	1.0	3.0	2.0	2.3	2.4	2.7	3.5
Ce	331.0	247.0	407.0	431.0	309.0	271.0	273.0	306.0	323.0
W		5.0			8.7	5.5	5.8	7.8	10.5
Th	18.0	0.4	14.0	10.0	14.0	16.0	15.0	12.0	18.0
U					5.4	4.3	6.3	3.6	5.9

[a] Glass inclusions 6, 11, 14, and 15 located on crack in host phenocryst. Glass inclusion 2 contains multiple voids (bubbles) or void space is 4 vol %.

[b] SiO_2 through Cl determined by electron microprobe; concentrations of SiO_2 through Cl have been normalized to give totals of 100% (anhyrous); total, actual electron microprobe totals in wt%. Total iron as FeO

[c] H_2O and Li through U determined by SIMS

[d] Indicates duplicate SIMS analysis

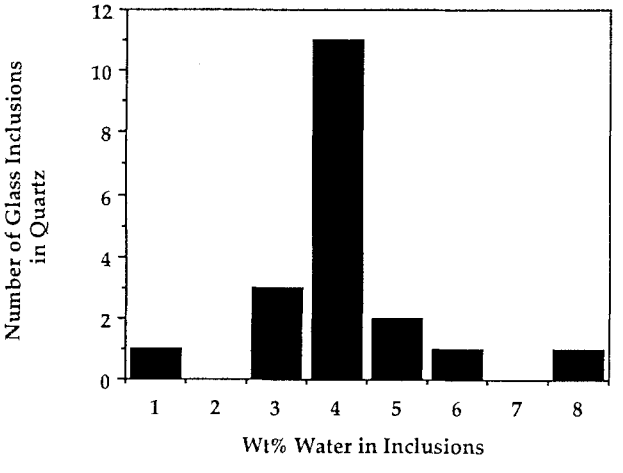

Fig. 1. Histogram showing number of glass inclusions, in quartz from samples AW-13 and AW-14, analyzed for water versus their water contents. On abscissa 1 is 0–1 wt%, 2 is 1–2 wt%, and so on

volatiles after entrapment. Inclusion 11 contains only 0.4 wt% H_2O and is in contact with a crack running through the host phenocryst. In addition, abundances of Li, Be, B, Mo, and Th are lower in this inclusion than those in other inclusions from this sample; thus, relatively volatile constituents in inclusion 11 apparently exsolved from the melt and escaped along the crack after trapping.

Four glass inclusions in anorthoclase phenocrysts from sample AW-13 were analyzed for major and minor elements (Table 5); one was also analyzed for H_2O. The glass inclusion compositions are highly variable and are different from those in quartz; inclusions in feldspar are comparatively enriched in SiO_2 and depleted in FeO, Al_2O_3, K_2O, and CaO. These differences are probably the result of amphibole crystallization after entrapment.

Discussion

Before applying the results to eruptive processes, the data were analyzed to identify and reject those inclusions whose compositions may have changed by processes occurring after melt entrapment. Glass inclusions whose compositions are suspect may not be chemically representative of melt, and these include devitrified inclusions, inclusions in contact with fractures, and inclusions containing relatively large bubble volumes. Suspect inclusions were not analyzed by SIMS, and they are not addressed further. An additional concern is whether or not the compositions of inclusions in quartz have been variably modified by post-trapping crystallization of quartz.

Table 4. Average compositions of glass inclusions in quartz and matrix glass

	AW-13				AW-14			
	Glass inclusions		Matrix Glass		Glassinclusions		Matrix glass	
	Mean[a] Concentration	± 1σ	Mean[b] Concentration	± 1σ	Mean[c] Concentration	± 1σ	Mean[d] Concentration	± 1σ
wt%								
SiO_2	71.17	0.67	73.87	2.31	70.82	0.81	73.92	0.39
Al_2O_3	8.98	0.51	9.03	2.29	9.33	0.83	8.29	0.25
CAO	0.32	0.04	0.24	0.06	0.31	0.05	0.28	0.01
Na_2O	6.41	0.36	6.13	0.04	6.43	0.78	6.23	0.34
K_2O	4.31	0.25	3.99	0.52	4.33	0.19	3.89	0.04
FeO	7.59	0.43	6.03	0.42	7.58	0.29	6.50	0.04
MgO	0.05	0.03	0.02	0.01	0.04	0.02	0.02	0.02
TiO_2	0.28	0.03	0.21	0.03	0.28	0.03	0.24	0.01
MnO	0.31	0.05	0.21	0.05	0.30	0.03	0.25	0.02
F	0.30	0.11	0.27	0.09	0.30	0.09	0.27	0.05
Cl	0.30	0.02	0.21	0.03	0.31	0.03	0.25	0.01
Totals	100.00		100.00		100.00		100.00	
H_2O	4.6[e]	0.7	0.2		4.9[f]	1.4	0.2	
ppm								
Li	65	20	53		72	14	53	
Be	10	1	8		10	1	7	
B	22	4	23		21	3	16	
Rb	220	55	166		190	19	167	
Sr	9	3	8		8	2	7	
Y	177	30	168		169	30	176	
Zr	2,073	393	2,368		2,094	419	2,541	
Nb	244	48	246		241	36	260	
Mo	9	3	nd		11	1	nd	
Sn	24	6	nd		24	3	nd	
Cs	3	1	2		2	0.8	8	
Ce	356	50	243		331	56	307	
W	7	1	nd		8	2	nd	
Th	14	4	nd		14	3	18	
U	5	1	nd		5	1	nd	

Totals have been normalized to 100% (anhydrous). Total iron as FeO; nd, no data collected

[a] Means and 1 σ for 14 glass inclusions for SiO_2 through H_2O and 10 analyses for Li through U

[b] Means and 1 σ for 3 matrix glass analyses for SiO_2 through H_2O. Only 1 analysis for Li through U; no precision reported

[c] Means and 1 σ for 14 glass inclusions for SiO_2 through H_2O and 8 analyses for Li through U

[d] Means and 1 σ for 5 matrix glass analyses for SiO_2 through H_2O. Only 1 analysis for Li through U

[e] Mean and 1 σ of 10 glass inclusion analyses

[f] Mean and 1 σ of 8 glass inclusion analyses (inclusion 11 apparently leaked after entrapment and was not included in the average)

Table 5. Compositions of glass inclusions in anorthoclase (sample AW-13)

	18	19	20	21
SiO_2	74.97	77.77	78.76	73.90
Al_2O_3	7.56	4.04	5.55	6.89
CaO	0.11	0.07	0.04	0.22
Na_2O	5.92	4.96	4.84	6.79
K_2O	3.71	3.17	3.26	3.46
FeO	6.19	7.69	6.39	7.24
MgO	0.05	0.06	0.04	0.06
TiO_2	0.48	0.42	0.38	0.56
MnO	0.24	0.42	0.35	0.36
F	0.47	0.21	0.13	0.21
Cl	0.27	0.32	0.26	0.31
H_2O	6.7	nd	nd	nd

Concentration in wt%. Analyses have been normalized to give anhydrous totals of 100 wt%; actual electron microprobe totals ranged from 94 to 97 wt%.
Total iron as FeO; nd, no data collected

Although we observe no textural evidence of secondarily precipitated quartz within the glass inclusions, the compositions of many inclusions suggest that small and variable amounts of silica crystallized from melt after entrapment. Most glass inclusions in quartz contain less silica than the matrix glasses, while nearly all other constituents analyzed are more enriched in inclusions than in matrix glasses (Table 4). Moreover, concentrations of CaO and K_2O in inclusions exhibit strong negative correlations with SiO_2 (Fig. 2). Silica exhibits inverse correlations with other major and minor constituent in glass inclusions, but the data exhibit more scatter and relationships are less clear.

These relationships have been used previously (Webster and Duffield 1991) to assess the degree of post-trapping quartz crystallization and determine the extent to which the constituents other than SiO_2 may have been secondarily enriched. We use the same method here. Assuming the Fantale melt contained 74 wt% SiO_2 (the

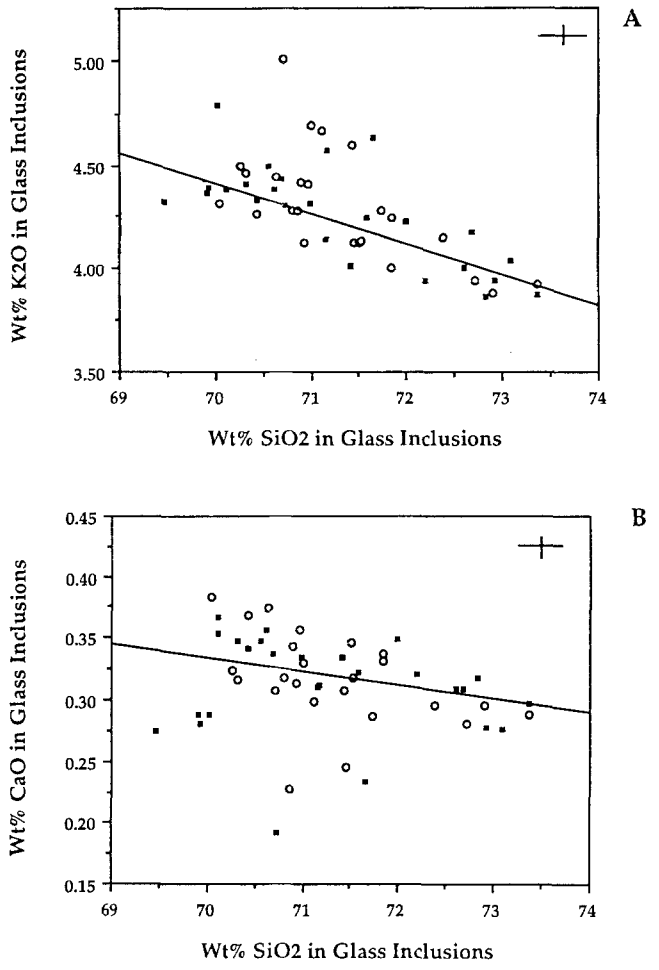

Fig. 2A, B. Concentrations of: **A** K_2O; **B** CaO versus SiO_2 in glass inclusions in quartz from samples AW-13, *circles*, and AW-14 *squares*; error bars are $\pm$ 1σ. The lines are the predicted decrease in SiO_2 and the increase in K_2O and CaO if quartz crystallized from trapped melt, assuming melt contained relatively low concentrations of K_2O and CaO and roughly 74 wt% SiO_2 at time of trapping. The agreement between predictive lines and data is good, suggesting that post-trapping quartz crystallization modified compositions of trapped melt

matrix glass contains roughly 74 wt% SiO_2, on average, and several inclusions contain SiO_2 concentrations approaching 73.5 wt% on an anhydrous basis), the *maximum* enrichment of constituents other than silica in glass of any individual glass inclusion is 13% relative, because the lowest concentration of silica in any single inclusion is roughly 70 wt%. The *average* concentrations of SiO_2 in glass inclusions decreased from 74 to 71 wt%; hence, the *maximum* extent to which the average concentrations of all constituents, other than SiO_2, may be artifically high is 10% relative. In comparison, the value of 10% relative is significantly greater than the analytical precision for the major- and minor-element analyses and is in the range of the analytical error for most trace elements.

Comparison of glass inclusion and whole-rock compositions

Trends observed in whole-rock data from Fantale show good agreement with those involving glass inclusions. Analysis of glassy rocks (Gibson 1970, 1974) from pre-, syn-, and post-caldera eruptive units shows that with increasing silica content, the concentrations of Cl, Rb, Zr, and Ce increase and concentrations of Sr and Ba decrease. The trace-element concentrations of glass inclusions in quartz also show distinct trends that reflect the evolution of the magma (Fig. 3); Rb, Y, Zr, Nb, and Ce increase with increasing differentiation. Concentrations of Cl in glass inclusions from sample AW-14 also increase with progressive differentiation.

Glass inclusion compositions indicate that samples AW-13 and AW-14 erupted from a highly evolved fraction of pantellerite magma; the magma was strongly enriched in water and high field strength cations, Zr, Ce, Nb, and Y. It is also noteworthy that no strong relationships occur

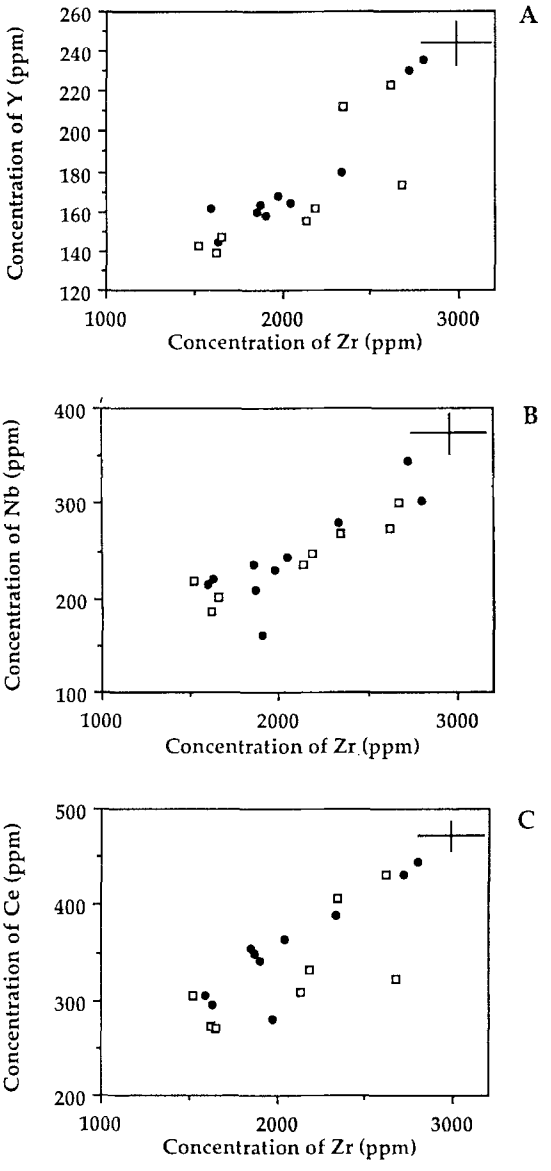

Fig. 3A–C. Concentrations of high-field strength cations: **A** Y; **B** Nb; **C** Ce versus Zr for glass inclusions in quartz from samples AW-13, *filled circles*, and AW-14, *open squares*; error bars are $\pm$ 1σ. The trace-element correlations reflect the differentiation of Fantale magma

between water and trace elements in the inclusions. The water content of inclusions does not increase with increasing abundances of high field strength cations, suggesting that some other process has affected the pre-eruptive water concentration of this fraction of magma. Water may have been lost to bubbles in inclusions. The trace-element data will be dealt within more detail in a companion paper.

Pre-eruptive water contents of Fantale magma

The H_2O concentrations of glass inclusions in quartz and feldspar indicate that this pulse of post-caldera, pantelleritic magma was enriched in H_2O, with an average pre-eruptive H_2O content of 4.8 wt%. The high apparent water contents are not an artifact of post-trapping quartz crystallization. If post-trapping quartz crystallization occurred, then melt that erupted to form sample AW-13 must have contained at least 4.2 wt% H_2O on average and melt erupted as AW-14 contained at least 4.4 wt% H_2O on average. It should also be kept in mind that the presence of crystals in inclusion bubbles suggests water may have been lost from trapped melt to the bubbles; the crystals may have precipitated from a fluid phase. Furthermore, the lack of correlation between trace-element and water concentrations of the inclusions also suggests that some water may have been lost from trapped melt.

Experimental studies concerned with crystallization of pantelleritic liquids are of little help in constraining pre-eruptive water contents of Fantale magma. Acmite is the liquidus phase in hydrous experiments conducted with $P_{H_2O} = 1$ kbar, followed by alkali feldspar and quartz (Carmichael and MacKenzie 1963; Thompson and MacKenzie 1967; Bailey and Cooper 1978). In contrast, experiments show that under relatively anhydrous conditions quartz is the liquidus phase followed by alkali feldspar, clinopyroxene, and alkali amphibole (Luth 1976). Presently, there are no published experimental data that constrain phase relations of pantelleritic melts containing intermediate water contents (i.e. pantelleritic liquids in equilibrium with a water-poor fluid or fluid-absent experiments that contain at least a percent of H_2O). As anorthoclase is the apparent liquidus phase of the obsidians of this study, all we can conclude from this comparison is that post-caldera pantelleritic magma at Fantale may not have been water-saturated at the time of entrapment.

The results of this study and of Kovalenko et al. (1988) present the interesting observation that post-caldera volcanic rocks from Pantelleria and Fantale were erupted from comparatively water rich fractions of magma. We suggest that future studies should determine if pre-eruptive water contents of alkaline and silicic pre-caldera rocks differ significantly from those of post-caldera rocks.

Degassing of magma and/or glassy flows at Fantale

We can constrain the effects of degassing of Fantale magma and cooling glassy flows by comparing compositions of glass inclusions, which represent trapped melt, with those of outgassed matrix glasses. At the 1σ confidence level (Table 4), the average concentrations of SiO_2 are higher in matrix glass of both rocks, and average concentrations of H_2O and Cl are lower in matrix glass (on an anhydrous basis). Furthermore, matrix glass of sample AW-14 is depleted in K_2O and MnO relative to those oxides in glass inclusions. If we account for the effects of post-trapping quartz crystallization, then the only statistically significant differences in composition between matrix glass and glass inclusions, at the 1σ confidence level, involve H_2O and Cl. Water and Cl were lost from melt some time after glass inclusions were trapped.

The exsolution of Cl and H_2O from pantellerite magma at Fantale may have begun under equilibrium conditions, and we have quantified the relative losses of H_2O and Cl to assess processes of vapor exsolution. The *total* masses of H_2O and Cl exsolved from melt are determined by simple mass balance computations. Each 100 kg fraction of melt exsolved a total of 0.06 kg of Cl and 4.55 kg of H_2O, based on the average concentrations of H_2O and Cl in glass inclusions and matrix glasses from both samples. If the volatiles exsolved as a single mass of vapor, and if we assume for simplicity that all chloride ions were associated with Na in the vapor, then the apparent *average* concentration of Cl in this vapor was 1.3 wt%. The Cl concentration of pantellerite melt ranged from 0.29 wt% (i.e., the maximum average value determined in the glass inclusions from both rock samples) at the onset of degassing to 0.21 wt% (i.e., the minimum average determined in matrix glass from both rock samples) as degassing waned. Hence, the apparent distribution coefficient for Cl (i.e., D_{Cl} = concentration of Cl in aqueous fluid/concentration of Cl in melt) ranges from approximately 4 to 6.

It is interesting to compare the apparent values of D_{Cl} for Fantale magma with those determined in experimental studies conducted with synthetic analogues. Recent experiments have determined the *equilibrium* distribution of Cl between aqueous fluid and peralkaline haplogranite melt having molar $(Na_2O + K_2O/Al_2O_3) = 1.7$ and molar $(Na_2O/Na_2O + K_2O)$ near 0.7 (Webster 1992). Fantale glass inclusions have nearly identical values for these compositional parameters; hence, the experimental glasses are similar in composition to glass inclusions, except that the inclusions contain significantly more FeO. At 800 °C and 2 kbar, which is the lowest P experimentally studied, D_{Cl} is roughly 10 if halogranite melt contains 0.21 wt% Cl and about 18 if melt contains 0.29 wt% Cl (Webster 1992). The apparent values of D_{Cl} that describe the exsolution of vapor at Fantale (i.e., 4–6) are lower than but similar to the experimentally determined values at 2 kbar (i.e., 10–18). The lower apparent values of D_{Cl} may be a function of the differences in P and T of volatile release or the difference in iron content (Metrich and Rutherford 1992) between the experimental glasses and the glass inclusions. Partitioning of Cl between melt and fluid varies strongly with P and T (Webster 1992). Hence, if fluid began to exsolve from Fantale magma near 800 °C and at P somewhat lower than 2 kbar, then the effect of lower P would reduce the distribution coefficient and may account for the observed differences in D_{Cl}. Alternatively,

fluid exsolution could have begun at 2 kbar and some T marginally greater than 800 °C, and the effect of the higher T would reduce the distribution coefficient and account for the differences in D_{Cl}. Thus, volatile exsolution may have begun at or near 2 kbar and 800 °C.

Although the release of Cl and H_2O from pantellerite magma at Fantale may have begun under equilibrium conditions, volatile exsolution may also have been influenced by the kinetics of diffusion during the end stages of magma ascent. It is clear that the release of water continued to very low P (i.e., less than 10 bars), due to the extremely low water concentrations in matrix glasses. Watzon (1990) demonstrated that the diffusion of Cl in a hydrous, metaluminous obsidian melt is slower than that of CO_2 and H_2O in experiments conducted at 10 kbar. He concluded that significant diffusive fractionation of H_2O, CO_2, and Cl may occur during vapor exsolution. We assume that Watson's (1990) experimental results for metaluminous melt at relatively high P also hold for peralkaline melts at shallow crustal P. Thus, when the H_2O- and Cl-rich, post-caldera pantellerite magma erupted at Fantale, the rate of cooling may have been slow enough to allow most of the water to escape, but not slow enough for Cl to achieve an equilibrium distribution between melt and vapor. The fact that a significant loss of water from melt occurred during and after eruption indicates that the quench rate must have been relatively rapid; otherwise, the exsolution of water vapor would have promoted extensive crystallization

It has been suggested that the pre-eruptive water contents of pantellerite magmas are low, based on the observation that concentrations of Cl in pantellerite matrix glasses are high. The underlying argument is that if a pantellerite magma is enriched in water and exsolves an aqueous vapor or fluid under equilibrium conditions, the fluid should remove a significant part of the Cl initially present in melt; glasses quenched from fluid-saturated pantellerite magma should be depleted in Cl. At the time this argument was used (Carmichael 1962), the experimental data regarding Cl partitioning between fluid and peralkaline melt were not available. We now know that under some conditions the distribution of Cl between peralkaline melt and aqueous fluid may not be *strongly* in favor of fluid (Webster 1992) and as a result, fluid-melt interaction may not scavenge a large fraction of the Cl held by melt. The computations described above show that the loss of a Cl-charged fluid from Fantale melt, under equilibrium conditions near 2 kbar and 800 °C, would have removed less than one-third of the Cl initially present in melt. Thus, one *cannot* accurately characterize the degassing of H_2O and Cl from peralkaline magma or, by implication, the pre-eruptive water contents of such magma, by simply determining the Cl contents of pantelleritic matrix glasses.

Conclusions

Glass inclusions occur in quartz, anorthoclase, and aenigmatite phenocrysts in a post-caldera glassy flow from Fantale volcano, Ethiopia. Major-element data suggest that post-trapping quartz crystallization may have caused minor changes in the composition of trapped melt. SIMS analysis of glass inclusions demonstrates that post-caldera pantellerite magma at Fantale was strongly enriched in H_2O prior to eruption. The average pre-eruptive H_2O concentration of *this melt fraction* was at least 4.8 wt% (given that water may have exsolved to bubbles after entrapment), which is significantly higher than is generally considered to occur in pantellerite magmas. We note, however, that other fractions of Fantale magma may have contained different volatile abundances prior to eruption.

Comparison of the compositions of glass inclusions and matrix glass helps to assess the extent of volatile loss and shows that Cl and H_2O exsolved from melt and/or cooling obsidian during and after eruption. The exsolution of vapor during eruption may have begun under equilibrium conditions at or near 2 kbar and 800 °C. Subsequently, as magma continued its ascent to the surface, the exsolution of volatiles may have been strongly limited by the kinetics of diffusion. Magma degassing and/or quenching may have been very rapid during the end stages of magma ascent, and H_2O may have diffused through melt quickly enough to form an aqueous vapor. The diffusion of Cl through melt may have been relatively slow, however, and most of the Cl that was originally in melt would have been retained by the magma and/or matrix glass after eruption.

Acknowledgements. The samples from Fantale were kindly provided by John Moore. The peralkaline obsidian rock samples and metaluminous rock powders used as trace-element standards were kindly provided by R. Macdonald and E. Christiansen, respectively. We appreciate discussions with R. Hinton and J. Craven at Edinburgh regarding ion-microprobe analysis. We appreciate reviews of an early version of the manuscript by J. Lowenstern and G. Mahood. The manuscript was reviewed for C.M.P. by R. Hervig and R. Macdonald; any errors in the study are our own. The ion microprobe facility at Edinburgh is funded by NERC grant GR3/5611; water standards for SIMS analyses were provided to the Edinburgh facility by E. Stolper. We gratefully acknowledge use of the McCrone Associates-Atlanta ion microprobe. This research was funded by N.S.F. Grant EAR-9017274 to J.D.W.

References

Bailey DK, Cooper JP (1978) Comparison of the crystallisation of pantelleritic obsidian under hydrous and anhydrous conditions. In: Prog in Exp Petrol, NERC Pub, Ser D 11, 230–233

Bailey DK, Hampton CM (1990) Volatiles in alkaline magmatism. Lithos 26:157–165

Bailey DK, Macdonald R (1975) Fluorine and chlorine in peralkaline liquids and the need for magma generation in an open system. Mineral Mag 40:405–414

Bailey DK, Macdonald R (1987) Dry peralkaline felsic liquids and carbon dioxide flux through the Kenya rift zone. Geochem Soc Spec Pub, 1:91–105

Blake S (1984) Volatile oversaturation during the evolution of silicic magma chambers as an eruption trigger. J Geophys Res 8:8237–8244

Carmichael ISE (1962) Pantelleritic liquids and their phenocrysts. Mineral Mag 33:86–113

Carmichael ISE, MacKenzie WS (1963) Feldspar-liquid equilibria in pantellerites: an experimental study. Am J Sci 261:382–396

Civetta L, Cornette Y, Gillot PY, Orsi G (1988) The eruption history of Pantelleria (Sicily Channel) in the last 50 ka. Bull Volcanol 50:47–57

Dickinson DR, Gibson IL (1972) Feldspar fractionation and anomalous Sr^{87}/Sr^{86} ratios in a suite of peralkaline silicic rocks. Geol Soc Am Bull 83:231–240

Ewart A, Taylor SR, Capp AC (1968) Geochemistry of the pantellerites of Mayor Island, New Zealand. Contrib Mineral Petrol 17:116–140

Gibson IL (1970) A pantelleritic welded ash-flow tuff from the Ethiopian Rift Valley. Contrib Mineral Petrol 28:89–111

Gibson IL (1974) A review of the geology, petrology, and geochemistry of the volcano Fantale. Bull Volcanol 38:791–802

Kovalenko VI, Hervig RL, Sheridan MF (1988) Ion microprobe analyses of trace elements in anorthoclase, hedenbergite, aenigmatite, quartz, apatite and glass in pantellerite: evidence for high H_2O contents in pantellerite melt. Am Mineral 73:1038–1045

Kovalenko VI, Hervig RL, Naumov VB, Solovova IP, Schauer S (1990) Fluids in melts from Pantelleria Island (abstract). In: VM Goldschmidt Conf Program Abstr, p 58

Lacroix A (1930) Les rockes hyperalcalines du massif du Fantale et du col de Balla. Mem Soc Geol Fr 14:89–102

Lowenstern JB, Mahood GA (1990) Low water and carbon dioxide contents in pantellerites: implications for eruptive style and petrogenesis of strongly peralkaline magmas (abstract). In: VM Goldschmidt Conf Program and Abstr, p 62

Lowenstern JB, Mahood GA (1991) New data on magmatic H_2O contents of pantellerites, with implications for petrogenesis and eruptive dynamics at Pantelleria. Bull Volcanol 54:78–83

Lowenstern JB, Mahood GA, Rivers ML, Sutton SR (1991) Evidence for extreme partitioning of copper into a magmatic vapor phase. Science 252:1405–1409

Luth WC (1976) Granitic rocks. In: Bailey DK, Macdonald R (eds) The evolution of the crystalline rocks. Academic Press, London New York Toronto, pp 335–417

Macdonald R, Bailey DK (1973) The chemistry of the peralkaline oversaturated obsidians. In: Data of geochemistry chapter N: chemistry of igneous rocks. Geol Surv Prof Pap 440-N-1

Macdonald R, Davies GR, Bliss CM, Leat PT, Bailey DK, Smith RL (1987) Geochemistry of high-silica peralkaline rhyolites, Naivasha, Kenya Rift Valley. J Petrol 28:979–1008

Mahood GA (1981) A summary of the geology and petrology of the Sierra La Primavera, Jalisco, Mexico. J Geophys Res 86:10131–10135

Mahood GA (1984) Pyroclastic rocks and calderas associated with strongly peralkaline magmatism. J Geophys Res 89:8540–8552

Mahood GA, Stimac JA (1990) Trace-element partitioning in pantellerites and trachytes. Geochim Cosmochim Acta 54:2257–2276

Metrich N, Rutherford MJ (1992) Experimental study of chlorine behavior in hydrous silicic melts. Geochim Cosmochim Acta 56:607–616

Mohr PA (1970) Volcanic composition in relation to tectonics in the Ethiopian rift system: a preliminary investigation. Bull Volcanol 34:141–157

Nicholls, J, Carmichael JSE (1969) Peralkaline acid liquids: a petrological study. Contrib Mineral Petrol 20:268–294

Rohleder HPT, Hitchen SC (1930) Vulkanologische Beobachtungen längs der Bahnlinie Adis Abebe-Djiboute (Abessinien). Z Vulk 12:269–289

Sparks RSJ (1978) The dynamics of bubble formation and growth in magmas: a review and analysis. J Volcanol Geothermal Res 3:1–37

Teillhard deChardin P, Lamarre P (1930) Le canon de L'aouache et le volcan Fantale. Mem Soc Geol Fr 14:13–20

Thompson RN, MacKenzie WS (1967) Feldspar-liquid equilibria in peralkaline acid liquids: An experimental study. Am J Sci 265:714–734

Watson EB (1990) Diffusion of dissolved carbonate and chlorine in water-bearing silicic magmas at 1 GPa and 800–1100 °C (abstract). In : VM Goldschmidt Conf Program and Abstr, p 89

Webster JD (1992) Fluid-melt interactions involving Cl-rich granites: experimental study from 2 to 8 kbar. Geochim Cosmochim Acta 56:659–678

Webster JD, Duffield WA (1991) Volatiles and lithophile elements in Taylor Creek rhyolite: constraints from glass inclusion analysis. Am Mineral 76:1628–1645

Webster JD, Holloway JR, Hervig RL (1987) Phase equilibria of a Be, U and F-enriched vitrophyre from Spor Mountain, Utah. Geochim Cosmochim Acta 51:389–402

Editorial responsibility: T. Grove